






Original Article


Soil chronosequence derived from landslides on the upper reach of Minjiang River, western China

HE Jun-bo^{1,2}  <https://orcid.org/0000-0002-4485-0758>; e-mail: hejunbo@imde.ac.cn

WU Yan-hong^{1*}  <https://orcid.org/0000-0002-9803-0544>;  e-mail: yhwu@imde.ac.cn

BING Hai-jian¹  <https://orcid.org/0000-0002-9813-6939>; e-mail: hjbing@imde.ac.cn

ZHU He¹  <https://orcid.org/0000-0001-8402-9692>; e-mail: zhuhe@imde.ac.cn

ZHOU Jun¹  <https://orcid.org/0000-0001-7315-6645>; e-mail: zhoujun@imde.ac.cn

* Corresponding author

¹ Institute of Mountain Hazards and Environment, Chinese Academy of Sciences, Chengdu 610041, China

² University of Chinese Academy of Sciences, Beijing 100049, China

Citation: He JB, Wu Yh, Bing HJ, et al. (2023) Soil chronosequence derived from landslides on the upper reach of Minjiang River, western China. *Journal of Mountain Science* 20(5). <https://doi.org/10.1007/s11629-022-7824-5>

© Science Press, Institute of Mountain Hazards and Environment, CAS and Springer-Verlag GmbH Germany, part of Springer Nature 2023

Abstract: Soil chronosequences derived from landslides with certain time series are the great avenue to elevate our understanding on the processes of pedogenesis, nutrient dynamics, and ecosystem evolution. However, the construction of reliable soil chronosequence from historical landslides remains intricate. Here, we presented a 22,000-year soil chronosequence from multiple landslides on the upper reach of Minjiang River, western China. The variation in a variety of pedogenesis indices and soil nutrients verified the reliability of the chronosequence. The silica-alumina ratio and silica sesquioxide ratio decreased significantly with soil age. This reflected the enrichment of Al/Fe/Ti oxides but the depletion of Si oxides with the soil development. Meanwhile, the values of the Chemical Index of Weathering and the Chemical Index of Alteration increased significantly with soil age, especially from 5 to 89 years. These variations were attributed to the soil weathering, which led to the destruction of soil minerals with the rapid loss of most of cations (e.g., K, Na, Ca, and Mg) during the soil development. The

concentrations of carbon and nitrogen in topsoil increased with soil age, and the carbon accumulation rate slowed significantly from 5,500 to 22,000 years. The total phosphorus concentrations decreased with soil age, suggesting the gradual loss of soil phosphorus with soil development. The results indicate that the landslide chronosequence established on the upper reach of Minjiang River is reliable and delineates a long-term soil development process, which will provide a great platform for further improvement of biogeochemical theories and understanding sustainable vegetation restoration.

Keywords: Soil chronosequences; Landslides; Weathering indices; Pedogenesis, Soil nutrients

1 Introduction

Landslides have seriously threatened the safety of mountain ecosystems worldwide (Ardizzone et al. 2007; Schlögel et al. 2015). However, landslides can strikingly accelerate nutrient cycling via soil development and sediment transport after the

Received: 14-Nov-2022
1st Revision: 22-Feb-2023
2nd Revision: 15-Mar-2023
Accepted: 05-May-2023

exposure of new rocks or parent materials (Hilton et al. 2011). Various landslide events are linked to severe weather that continues to expand through climate change in many regions of the world, while the mechanisms of mutual feedback between landslides, biosphere and climate remain unclear (Walker et al. 2010; Schulz et al. 2013; Błonska et al. 2018; Hemingway et al. 2018; Olivia and Dirk 2022). Soil chronosequences derived from landslides have a great potential to explore soil development and nutrient dynamics because of the well-recorded soil age and successive vegetation development. This can not only elevate the understanding of the interaction of landslides with climate and biosphere, but also improve the theory of primary succession. Therefore, it is the priority to construct a reliable soil chronosequence from historical landslides, especially for a long-term temporal scale.

Soil chronosequences are soil continuums with changes in vegetation, topography, and climate (Jenny 1969; Harden 1982). The concept of “space for time” in a chronosequence allows examining the relationships among soil development, vegetation succession, weathering, and geomorphological processes (Stevens and Walker 1970; Yaalon 1983; Huggett 1998; Beilke et al. 2013). The key to constructing a chronosequence is to clarify soil ages, which ensures that the chronosequence represents a successive stage of one or several pedogenic processes (Rode 1961; Vreeken 1975; Huggett 1998). Based on the viewpoint, one of the most popular methods in constructing chronosequences on the known age soils (Birkeland 1990). Sites such as coastal sand dunes, lava flows, moraines, and landslides provide soils of the known ages, which are ideal for constructing soil chronosequences. Several soil chronosequences have been studied, such as the iconic Franz Josef post-glacial chronosequence (Walker and Syers 1976), basaltic chronosequence along the Hawaiian Islands (Crews et al. 1995), the Northern Arizona Volcanic Field chronosequence (Selmants and Hart 2010), marine sedimentary chronosequence along the Mendocino Terrace (Izquierdo et al. 2013), coastal sand dunes chronosequence at Haast, New Zealand (Turner et al. 2012), coastal sand dunes chronosequence at Jurien Bay, Western Australia (Turner and Laliberté 2015), and a post-glacial chronosequence at Hailuogou, Southwestern China (Wu et al. 2015). However, long-term landslide soil chronosequence is rare. Most chronosequences

derived from landslides were short-term and dated back hundreds of years ago (Olivia and Dirk 2022). Short-term landslide chronosequences are mainly formed on several adjacent landslides, and the time when the landslides occurred is accurately recorded (Hilton et al. 2011; Ramos et al. 2012; Błonska et al. 2018; Hemingway et al. 2018). It is relative to the short-term landslide chronosequences with the accurate age (Guzzetti et al. 2012; Razak et al. 2013; Vindusková et al. 2019) challenging to construct a long-term landslide chronosequence.

A standard method to construct a long-term landslide chronosequence is based on geological chronology (Bronk 2009; Reimer et al. 2013; Olivia and Dirk 2022), and the indices of soil development and the characteristics of soils at different ages can be used to verify the reliability of a chronosequence. The indices of soil development include silica-alumina ratio (Sa), silica sesquioxide ratio (Saf) (Zhao et al. 1983; Alexandre et al. 1997; Huang et al. 2002; Derry et al. 2005), chemical index of weathering (CIW), and chemical index of alteration (CIA) (Birkeland 1974; Guggenberger et al. 1998; Daniel et al. 2001; Huang and Gong 2001; Martha et al. 2008). The values of Sa and Saf can indicate the processed silicon (Si) loss and aluminum (Al) enrichment in soils (Zhao et al. 1983), and extensive research showed the decreased values of Sa and Saf with soil development (Parker 1970; Zhao et al. 1983; Alexandre et al. 1997; Huang et al. 2002; Derry et al. 2005). Yang et al. (2010) found that the values of Sa and Saf increased slowly at the later stages of soil development. The indices of CIW and CIA, the ratios of Al_2O_3 to unstable oxides, have been widely used to evaluate the chemical weathering strength of feldspar quantitatively (Nesbitt and Young 1982; Yang et al. 2010). The higher values of CIA and CIW exist, the more elements such as K, Na, and Ca in silicate minerals are apt to be leached from the parent materials (Nesbitt and Young 1984). Moreover, the changes in soil carbon (C) during soil development have been extensively studied on both decadal and centennial scales (Lugo and Brown 1993; Post and Kwon 2000; Poeplau et al. 2011; Yang et al. 2016). Current research has established that soils eventually reach a specific soil C saturation capacity during soil development. In other words, further C inputs do not lead to the accumulation of C in the soil at later stages of soil development (Peltzer et al. 2010; Newman et al. 2020). The concentrations of nitrogen (N) were

significantly correlated with soil age, and many terrestrial ecosystems are devoid of N at the beginning of the succession (Walker and Syers 1976; Dahlgren 1994; Holloway and Dahlgren 2002). Accordingly, biological processes in many ecosystems on young soils may be limited by low supplies of N, but soil N concentrations increase rapidly with soil development (Vitousek and Farrington 1997; Newman and Hart 2015). Moreover, total phosphorus (Pt) concentrations also showed a significant relationship with soil age (Walker and Syers 1976; Kouno et al. 1995; Wardle et al. 2004). The Pt concentrations increased at the early stages of soil development, decreasing rapidly with soil development (Wu et al. 2015; Vindušková et al. 2019).

The study area is located in western China, and the unique physical geography and geological environment make it one of the areas in China with the highest occurrence rate, the most extensive scope, the most types, the highest frequency, and the worst effect of landslides and debris flows (Lu et al. 2021). This provides an ideal site for constructing a landslide soil chronosequence. We selected fourteen landslides with short-term sequences with long-term geological dating methods to construct a 22,000-year landslide soil chronosequence on the upper reach of Minjiang River, western China. To verify the reliability of the chronosequence, we investigated various indices of soil development (e.g., Sa, Saf, CIA, and CIW) and the concentrations of soil C, N, and P with different soil ages. If the values of Sa and Saf decreased along the chronosequence, and the values of CIW and CIA increased along the chronosequence, it represented the changes in soil properties along the chronosequence following the pedogenesis rule. We expected that the changes in the concentrations of topsoil C, N, and P along the chronosequence followed the patterns that soil C and N accumulate rapidly at the early stages of soil development. The concentrations of soil Pt increased with soil age at the early stages of soil development and then decreased with soil development.

2 Materials and Methods

2.1 Study area and soil sampling

The study area (103°32'-104°15'E, 30°45'-30°09'N) is located on the upper reach of Minjiang

River, eastern Tibetan Plateau (Fig. 1). The climate in the study area is dominated by an arid river valley climate (Fang et al. 2003). The mean annual temperature is 12°C, the mean annual precipitation is approximately 700 mm, with most of the precipitation occurring in the summer, and the annual evaporation is 1725 to 2,570 mm (Fang 1994). The mountains are the dominant landform in the study area, with elevation ranges of 762-5,963 m (Fig. 1). The parent rocks in the study area are dominated by sandstone and conglomerate (Table 1). Since the Cenozoic, the Tibetan Plateau has been a geologically active region uplifted by the collision between the Eurasian and Indian plates (Han et al. 2015; Zhong et al. 2022). This results in complicated geological conditions, frequent geological hazards, and a fragile ecological environment in the study area (Lu et al. 2021).

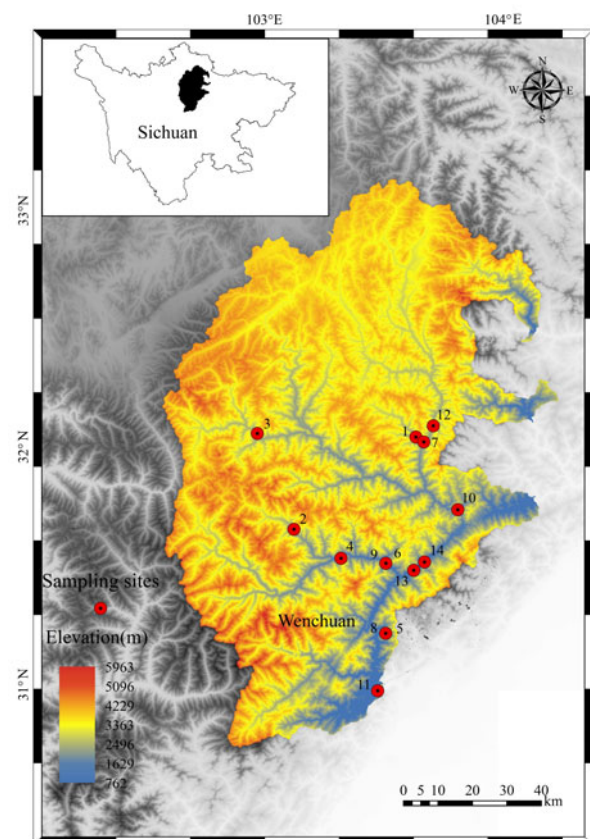


Fig. 1 Study area and sampling sites in the upper reach of the Minjiang River in Sichuan province of western China.

In total, 14 landslide sites were selected where landslides occurred 5 to 22,000 years before (Table 1). Soil samples were derived from landslides wholly reset by the landslide event. In order to select

Table 1 The basic characteristics of the study area

ID	Full name	Age (y) ^a	Location		Altitude (m)	Sampling area	Predominant parent rock	pH	Age published first in
			Longitude (E, °)	Latitude (N, °)					
1	Xinmo	5	103.655140	32.068647	2250	headscarp	sandstone/conglomerate	8.53	Xu et al. 2017
2	Tasi	12	103.143368	31.679613	2100	headscarp	sandstone/conglomerate	8.36	Gan et al. 2015
3	Luhua	15	102.989604	32.083414	2350	headscarp	sandstone/conglomerate	8.38	Wang et al. 2007
4	Jianshan	42	103.340866	31.557639	1900	headscarp	sandstone/conglomerate	7.92	Xie et al. 2004
5	Fotangba2	58	103.528527	31.241238	1670	headscarp	Sandstone	7.78	Xie et al. 2004
6	Chayuan2	74	103.529226	31.536676	1350	headscarp	sandstone/conglomerate	7.72	Wang et al. 2011
7	Diexi	89	103.688266	32.047831	2325	headscarp	Claystone	7.94	Nie et al. 2004
8	Fotangba1	110	103.528527	31.241238	1670	headscarp	sandstone/conglomerate	7.19	Xie et al. 2004
9	Chayuan1	134	103.529226	31.536676	1350	headscarp	sandstone/conglomerate	7.72	Wang et al. 2011
10	Huahong	300	103.831129	31.762311	1810	headscarp	Sandstone	6.99	Chai 2002
11	Shimenkan	1000	103.494763	30.999352	1510	headscarp	Conglomerate	7.14	Chai et al. 1995
12	Qiangyang	5500	103.728402	32.115634	2180	headscarp	sandstone/conglomerate	7.11	An et al. 2008
13	Koushan	14000	103.645949	31.506586	1500	headscarp	Conglomerate	7.08	Chai et al. 1995
14	Wenzhen	22000	103.691390	31.542233	1825	headscarp	sandstone/conglomerate	7.15	Wang et al. 2007

landslides without apparent disturbance from soil erosion and human activity, we avoided sampling on large intact landslide blocks, where lower central parts were preferred (Table 1). All sampling sites were selected in flat and similar topographic positions. At each sampling site, we established a representative 10 × 10 m plot and collected soil samples from the surface horizon (0-10 cm) and C horizon. Each soil sample was composed of three random sub-samples. The litter layers were removed when collecting the soil in the surface horizon. Due to high rock content in the C horizon, larger rocks (>5 cm) and soil were weighed separately, and a representative soil sample of about 1kg was taken for laboratory analyses. Their volume was estimated and recorded when the pit contained large rocks that could not be easily extracted from the pit. Another undisturbed core sample was collected by steel cylinders (100 cm³) to measure soil bulk density. Before analysis, plant roots and rock gravels were removed, and the fresh soil sample was passed through a 2 mm sieve and divided into two sub-samples. One was kept at 4°C for the analysis of soil C, N, and P. The other was air-dried for the analysis of the soil physical and chemical properties.

2.2. Physical and chemical analysis

Values of pH of soil samples were measured by a pH monitor (HACH HQ30D, USA) with a ratio of soil to water of 1:2.5 (w/v). In the soil samples, the concentrations of major elements (e.g., Al, Ca, Fe, K, Mg, Mn, Na, and Ti) were measured by an American Leeman Labs Profile inductively coupled plasma atomic emission spectrometer (ICP-AES). The soil C and N concentrations were measured by Elementar

Vario ISOTOPE cube (EA-IRMS, Germany). The concentrations of soil Pt were measured after acid digestion (HNO₃, HClO₄) by the molybdenum blue method using spectrophotometry at 889 nm (Murphy and Riley 1962).

2.3 Indices of soil development

The general index of soil development can clarify the degree of soil development (Janzen et al. 2011). The values of Sa and Saf can indicate the processed silicon (Si) loss and aluminum (Al) enrichment in soils (Huang 1996), which are empirically represented as:

$$Sa = \frac{SiO_2}{Al_2O_3} \quad (1)$$

$$Saf = \frac{SiO_2}{Al_2O_3 + Fe_2O_3} \quad (2)$$

Degree of weathering is classified based on CIA value, i.e., if the CIA value is between 40 and 66, the samples are low to moderately weathered, whereas if it exceeds 66, the samples are extensively weathered (Nesbitt and Young 1982; Harnois et al. 1988). This suggests the effective transformation of rock into soil by chemical alteration forming secondary minerals, i.e., clay minerals. CIA is represented by the below-mentioned empirical formula calculated by using molar proportion:

$$CIA = 100 \times \left[\frac{Al_2O_3}{Al_2O_3 + CaO + Na_2O + K_2O} \right] \quad (3)$$

We have also calculated the value of the chemical index of weathering (CIW) using the molar proportion, which is empirically represented as:

$$CIW = 100 \times \left[\frac{Al_2O_3}{Al_2O_3 + CaO + Na_2O} \right] \quad (4)$$

2.4. Statistical analysis

Before data analysis, all the data were checked for normality and logarithmically converted if necessary. Only a regression model using the age of landslide as a single predictor and providing the best fit in the figures. All parameter coefficients were normalized using a z-score conversion to make the parameter estimates comparable. Both independent samples t-test and Kruskal-Wallis test were conducted in SPSS 19.0 (IBM SPSS, USA), while other statistical analyses were conducted in R version 4.0.5 (R Core Team 2020).

3 Results

3.1 Soil chronosequence derived from landslides on the upper reach of the Minjiang River

There were significant differences in the soil properties along the chronosequence. In soil aged 5 to 74 years, the soil depth varied between 5 and 20 cm, dominantly composed of sand (58%-73%), the soil color was yellowish brown, and the mean value of soil pH was 8.12. The land covers transited from bare land to herbaceous plants (Fig. 2). In soil aged from 74 to 1000 years, the soil depth was 25 to 40 cm major composed of silt (53%-58%), the soil color is dark brown, and the mean value of soil pH was 7.46. During this period, the land covers transited from herbaceous plants to woody plants (Fig. 2). For the soil aged from 1,000 to 22,000 years, the thickness was 40 to 300 cm, the color was blackish brown, the mean value of pH was 7.12, and silt (59%-74%) was the major composition, of the land covers were herbaceous and woody plants (Fig. 2).

3.2 Indices of soil development

The Sa values varied between 0.017 and 0.023 (Fig. 3a), while the values of Saf were between 0.010 and 0.013 (Fig. 4a) in C horizon. For the topsoil, the Sa values were 0.0040 to 0.0203 and decreased with soil age (Fig. 3b). The topsoil had Saf values of topsoil also decreased from 0.0024 to 0.0128 with the soil age (Fig. 4b). The CIA obviously increased with soil age in the topsoil (Fig. 5a), while it changed a little in C horizon (Fig. 5b). The CIW had a similar change as CIA both in the topsoil (Fig. 6a) and C horizon (Fig. 6b).

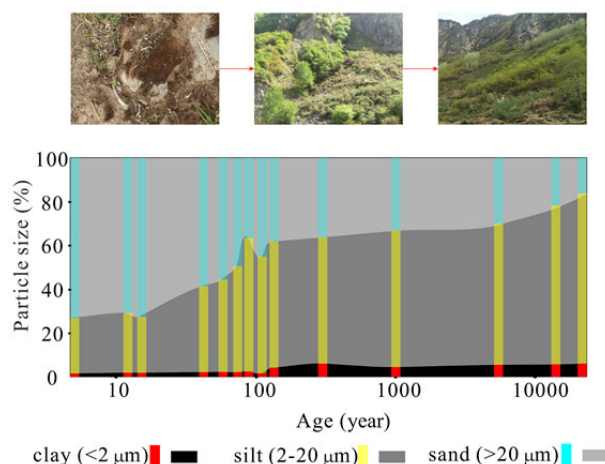


Fig. 2 Plants cover succession (upper) and changes in particle size composition (lower) along the landslide soil chronosequence on the upper reach of Minjiang River, western China.

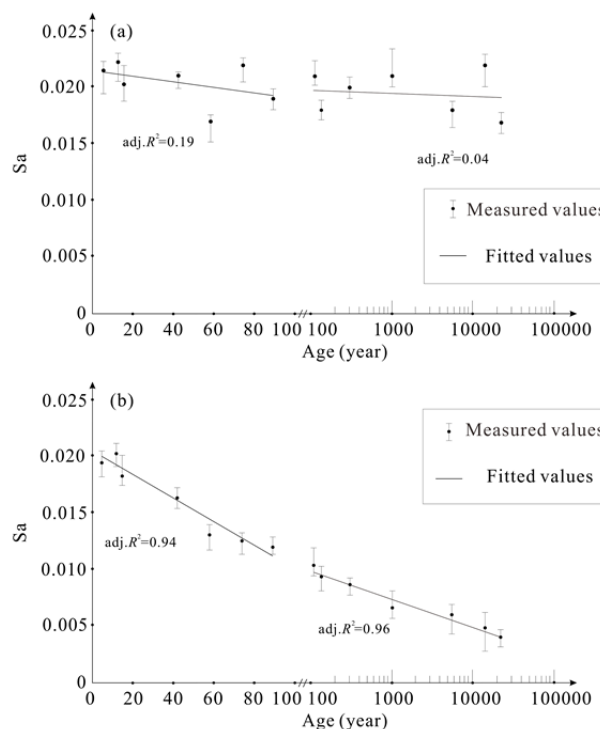


Fig. 3 Changes in the indices of Sa along the landslide soil chronosequence on the upper reach of Minjiang River, western China. The values are means \pm SE, $n=3$. (a) Values of Sa in C horizon soil; (b) Values of Sa in topsoil.

3.3 Carbon, nitrogen, and phosphorus concentrations and their stocks in topsoil

The concentration of C in the topsoil increased with soil age from 2.67 to 16.19 g/kg and more rapidly

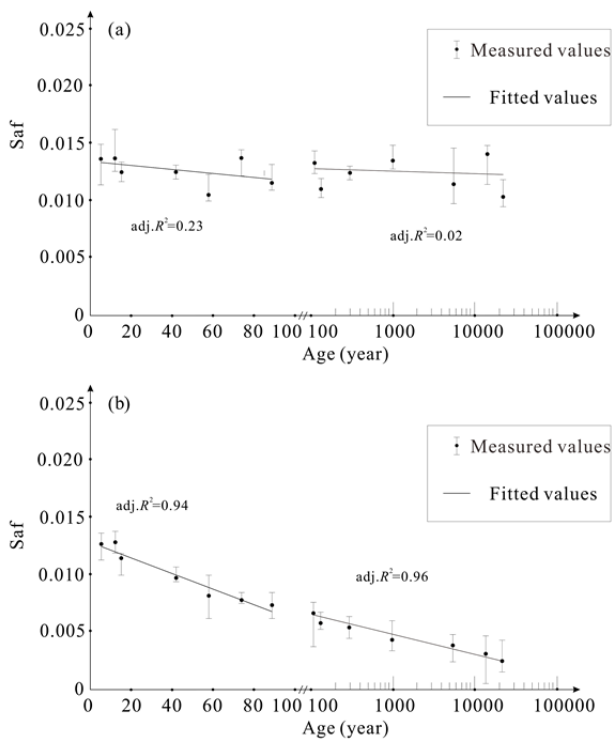


Fig. 4 Changes in the indices of Saf along the landslide soil chronosequence on the upper reach of Minjiang River, western China. The values are means \pm SE, $n=3$. (a) Values of Saf in C horizon soil; (b) Values of Saf in topsoil.

increased before 5500 years (Fig. 7a). The concentrations of N in the topsoil had a similar trend as C and increased from 0.2 to 1.8 g/kg (Fig. 7b). The Pt concentrations varied between 0.13 and 1.16 g/kg and showed a decreasing trend with the soil developed (Fig. 7c).

The stocks of C, N, and P of topsoil were calculated per square meter's contents with 10 cm soil depth, bulk density, and concentrations. The stocks of C and N increased from 0.21 kg/m² to 1.34 kg/m² (Fig. 8a) and 0.11 kg/m² to 0.15 kg/m² (Fig. 8b), respectively. Both stocks of C and N showed increased trends with the soil age. In contrast, stocks of P decreased significantly with soil age, from 0.086 kg/m² to 0.011 kg/m² (Fig. 8c). It implied that about 84% of phosphorus in the topsoil was lost during the soil development.

4 Discussion

4.1 Validation of landslide soil chronosequence by weathering indices

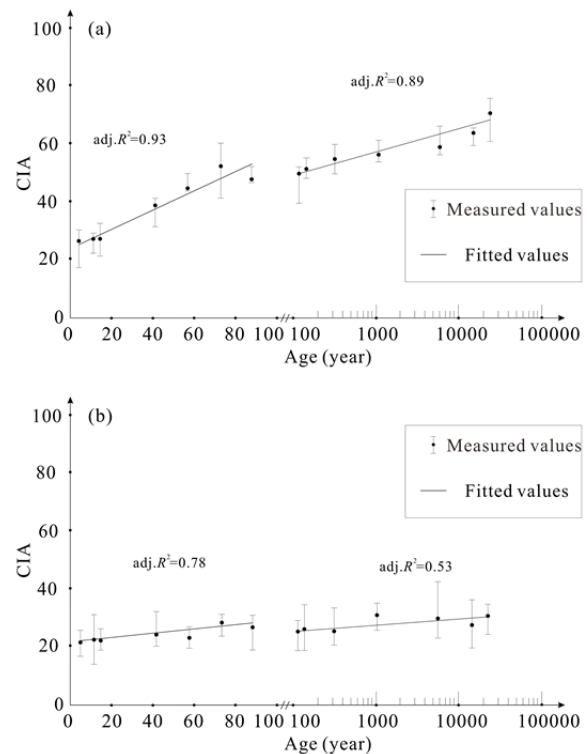


Fig. 5 Changes in the indices of CIA along the landslide soil chronosequence on the upper reach of Minjiang River, western China. The values are means \pm SE, $n=3$. (a) Values of CIA in topsoil; (b) Values of CIA in C horizon soil.

The values of the Sa and Saf in soil C horizon were uncorrelated with soil age (Fig. 3a, 4a), and they have no significant difference along the chronosequence. It demonstrated that the parent rock for soil development might have similar silica-alumina and silica sesquioxide ratios. Meanwhile, the approximations of CIW and CIA in soil C horizon along the chronosequence (Fig. 5b, 6b) indicated that the soil parent materials at each landslide might have a similar degree of weathering. However the early stages of soil development (soil age < 100 years), the values of the CIW and CIA in soil C horizon were remarkably correlated with soil age (adj. R^2 0.92, 0.78 respectively; Fig. 5b, 6b), but the correlation weakened at the later stages (soil age > 100 years) (adj. R^2 0.53, 0.40 respectively, Fig. 5b, 6b), suggesting that their relationship with soil age is not linear along the whole chronosequence, and the C horizon might be impacted by leaching of elements from topsoil as soil developed.

The changes in the values of CIA and CIW in the topsoil were consistent with our hypothesis (Fig. 5a, 6a). In the study area, frequent earthquakes and

intermittent neotectonics movements have led to rapid soil weathering, which might favor the leaching of mobile elements (Xu et al. 2017). As the soil developed, the differences between the values of the CIW and CIA of the topsoil from the C horizon increased significantly, further indicating that the intensifying weathering along the chronosequence (Fig. 5, 6), which resulted in the significant loss of most of the K, Na, Ca, and Mg with time. The values of the Sa and Saf in topsoil were significantly correlated with soil age (Fig. 3b, 4b) along the chronosequence. The changes in the values of Sa and Saf in the topsoil indicated the loss of Si and the accumulation of Fe and Al during pedogenesis. Typically, the release of ash elements (including Si) from plants and returning into the soil at the later stages of development decreases the loss of soil Si, resulting in a slower rate of decrease in the values of Sa and Saf (Yang et al. 2010). In our study, the values of Sa and Saf still showed a rapidly decreasing trend (Fig. 3b, 4b), implying that the amount of bio-silicon returned by plants was insufficient because of the lower litter decomposition rate caused by the arid climate.

Generally, soil properties varied along the chronosequence following the pedogenesis rule. Weathering indices changed smoothly with the soil development in 14 landslide sites without any remarkable abnormal variation along the soil chronosequence, which verified the reliability of the chronosequence.

4.2 Validation of landslide soil chronosequence by soil indicators

The changes in the concentrations of topsoil C along our chronosequence followed the patterns reported in previous studies that soil C concentrations reach a specific saturation capacity during soil development and further C inputs afterward do not lead to the accumulation of C in soil (James 1988; Hassink 1997; Stewart et al. 2007). In our soil chronosequences, soil C concentrations and stocks reached their saturation around 5,500 years (Fig. 7a, 8a). However, the long-term capacity of soils to store carbon and the rate at which soils approach this capacity remains to be determined (Six et al. 2002).

Rapid N accumulation occurs at the early stage of soil development when N is fixed biological fixation (Vitousek et al. 2004). After the rapid increase, soil N

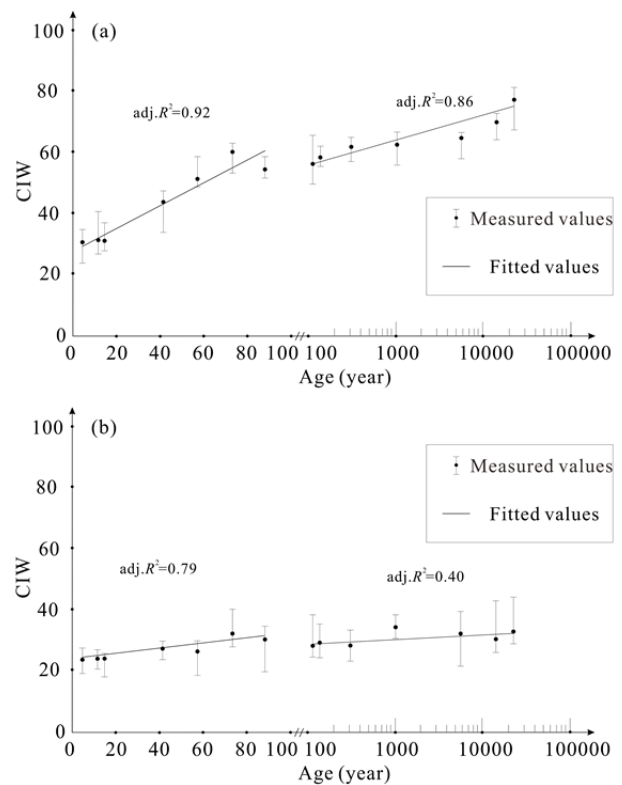


Fig. 6 Changes in the indices of CIW along the landslide soil chronosequence on the upper reach of Minjiang River, western China. The values are means \pm SE, $n=3$. (a) Values of CIW in topsoil; (b) Values of CIW in C horizon soil.

concentrations continuously increases till a certain peak (Lugo and Brown 1993; Post and Kwon 2000; Poeplau et al. 2011; Yang et al. 2016). The concentrations and stocks of topsoil N in the chronosequence demonstrated a rapid increase at the early stage and kept the increase trends afterward (Fig. 7b). No decrease trends of N concentration and stocks emerged in 22,000 years at the landslide sites, which might be attributed to unique N cycling in the study area. The weak correlation of topsoil Pt with soil age at the early stages of soil development (Fig. 7c) might be due to the rapid weathering and soil erosion that disturbed soil development (Wu et al. 2015). In the long term, the concentrations of topsoil Pt were negatively correlated with soil age (Fig. 7c), which might be resulted from the continuous loss of P. Overall, the changes in the concentrations of soil Pt along the chronosequence were in line with the dynamic pattern of soil Pt during pedogenesis (Walker and Syers 1976; Kouno et al. 1995; Wardle et al. 2004; Wu et al. 2015).

The temporal patterns of topsoil C, N, and P

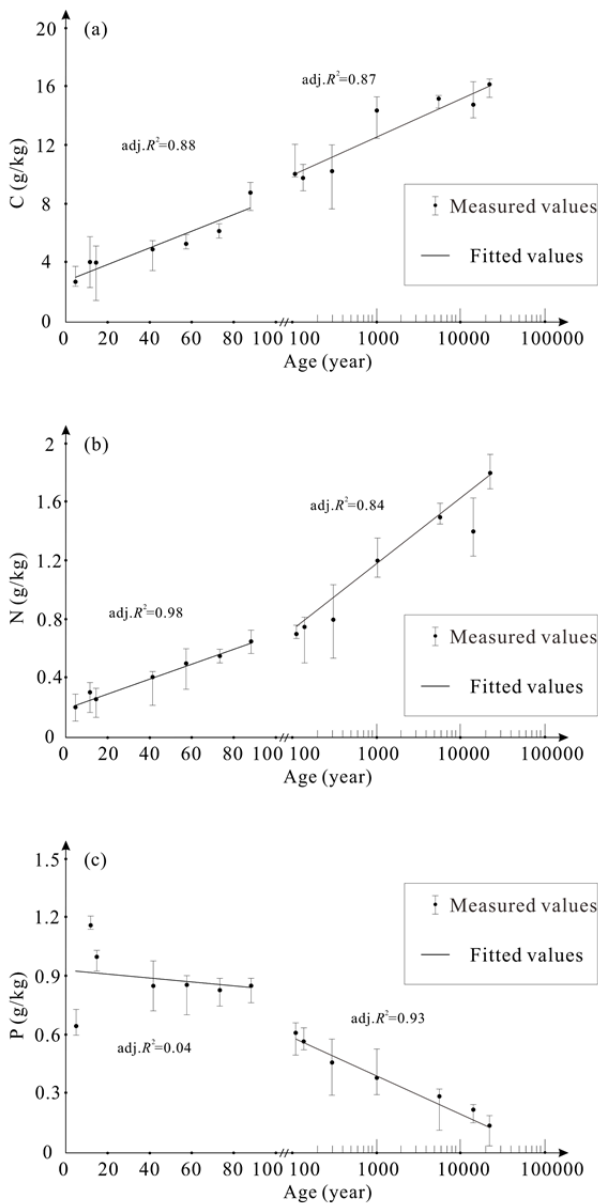


Fig. 7 Changes in the concentrations of topsoil C, N, and P along the landslide soil chronosequence on the upper reach of Minjiang River, western China. The values are means \pm SE, $n=3$. (a) Concentrations of total C; (b) Concentrations of total N; (c) Concentrations of total P.

stocks in topsoil along the soil chronosequence (Fig. 8) were similar to those observed for other long-term chronosequences (Crews et al. 1995; Wardle et al. 2004; Turner and Laliberté 2015; Vinduřková et al. 2019). These patterns were consistent with the result of the database analysis on the C, N, and P transformation as a function of pedogenesis (Yang and Post 2011), which further verified the reliability of the chronosequence.

The topsoil total C stocks came to a steady state

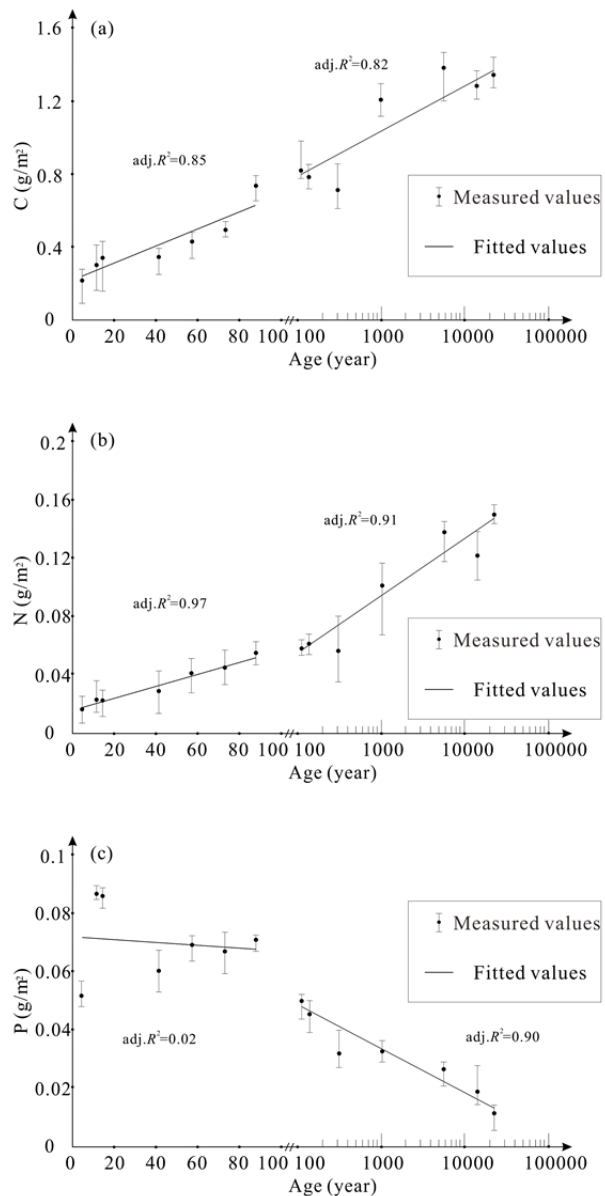


Fig. 8 Changes in the stocks of C, N, and P of topsoil along the landslide soil chronosequence on the upper reach of Minjiang River, western China. The values are means \pm SE, $n=3$. (a) Stocks of C of topsoil; (b) Stocks of N of topsoil; (c) Stocks of P of topsoil.

440 years after dune formation in Lake Michigan (Lichter 1998) and 566 years in Mt. Shasta volcanic mudflows (Dickson and Crocker 1953). In the chronosequence, the total C stocks in the topsoil maintained a slower increase or a relatively steady accumulation rate around 5,500 years (Fig. 8a). The possible interpretation for this lag is that the dry climate in the study area resulted in a slower succession of vegetation, lower productivity, and slow decomposition of litter. The rate of decreasing topsoil

Pt stocks in soil age from 100 to 22,000 years was much faster than other chronosequences (Fig. 8c) might be attributed to the steep slope of the study area (Wu et al. 2015).

In summary, the changes in soil C, N, and P in 14 landslide sites were similar to other soil chronosequences, which further verified the reliability of the landslide chronosequence. The decreased pH value trends and particle size composition variation also demonstrated this coherence.

5 Conclusion

In this work, a 22,000-year soil chronosequence was constructed using 14 landslides on the upper reach of Minjiang River, western China, based on the assumption that the time of landslides occurred was the beginning of the pedogenesis. However, the study area is frequently subject to geological hazards, which disturbed the soil development. The values of CIW, CIA, Sa, and Saf in C horizon for each landslide is similar, which supports that the selected landslides had similar soil parent rocks. As the soil develops, in the topsoil, the values of CIW, CIA increased, and the

values of Sa, Saf decreased. The variation trends of CIW, CIA, Sa, and Saf verified the reliability of the chronosequence. Topsoil C and N concentrations and stocks increased with soil age while those of P decreased, which followed the pedogenesis rules and supported the construction of chronosequence. Overall, this study validates a long-term soil chronosequence derived from landslides. These contribute to quantifying the impact of climate and environmental variables on soils, which not only allows for a better understand the factors driving soil development, but also to help foresee potential limitations in the provision of ecosystem services in the future derived from current rates of land degradation and climate change.

Acknowledgments

The research reported in this manuscript is funded by the Key Program of the Chinese Academy of Sciences for International Cooperation (131551KYSB20190028) and the Key Research and Development Projects Foundation of Sichuan, China (Grants No. 2018JZ0075).

References

- Alexandre A, Meunier JD, Colin F, et al. (1997) Plant impact on the biogeochemical cycle of silicon and related weathering processes. *Geochim Cosmochim Acta* 61(3): 677-682. [https://doi.org/10.1016/S0016-7037\(97\)00001-X](https://doi.org/10.1016/S0016-7037(97)00001-X)
- An WP, Zhao JQ, Yan XB, et al. (2008) Tectonic deformation of lacustrine sediments in Qiangyang on the Minjiang fault zone and ancient earthquake. *Seismology and Geology* 30(4): 980-988. (In Chinese).
- Ardizzone F, Cardinali M, Galli M, et al. (2007) Identification and mapping of recent rainfall-induced landslides using elevation data collected by airborne lidar. *Nat Hazards Earth Syst Sci* 7(6), 637-650. <https://doi.org/10.5194/nhess-7-637-2007>
- Beilke AJ and Bockheim JG (2013) Carbon and nitrogen trends in soil chronosequences of the Transantarctic Mountains. *Geoderma* 197: 117-125. <https://doi.org/10.1016/j.geoderma.2013.01.004>
- Birkeland PW (1974) *Pedology, weathering, and geomorphological research*. New York: Oxford University. pp 81-181.
- Birkeland PW (1990) Soil-geomorphic research-a selective overview. *Geomorphology* 3(3-4): 207-224. [https://doi.org/10.1016/0169-555X\(90\)90004-A](https://doi.org/10.1016/0169-555X(90)90004-A)
- Blonska E, Lasota J, Piaszczyk W, et al. (2018) The effect of landslide on soil organic carbon stock and biochemical properties of soil. *J Soils Sediments* 18 (8): 2727-2737. <https://doi.org/10.1007/s11368-017-1775-4>
- Bronk RC (2009) Bayesian analysis of radiocarbon dates. *Radiocarbon* 51(1): 337-360. https://doi.org/10.2458/azu_js_rc.51.3494
- Chai HJ, Liu HC (2002) Study on landslide damming of river in upper of Minjiang river. *J Mt Sci* 20(5): 616-620(In Chinese).
- Chai HJ, Liu HC, Zhang ZY (1995) The catalog of Chinese landslide dam events. *J Hazard Mater* 4: 1-9 (In Chinese).
- Crews TE, Kitayama K, Fownes JH, et al. (1995) Changes in soil phosphorus fractions and ecosystem dynamics across a long chronosequence in Hawaii. *Ecology* 76(5): 1407-1424. <https://doi.org/10.2307/1938144>
- Dahlgren RA (1994) Soil acidification and nitrogen saturation from weathering of ammonium-bearing rock. *Nature* 368(6478): 838-841. <https://doi.org/10.1038/369340co>
- Daniel RM (2001) Evolution of Soils on Quaternary Reef Terraces of Barbados, West Indies. *Quat Res* 56(1): 66-78. <https://doi.org/10.1006/qres.2001.2237>
- Derry LA, Kurtz AC, Ziegler K, et al. (2005) Biological control of terrestrial silica cycling and export fluxes to watersheds. *Nature* 433(7027):728-731. <https://doi.org/10.1038/nature03299>
- Dickson BA, Crocker RL (1953) A chronosequence of soils and vegetation near mt shasta, california .2. the development of the forest floors and the carbon and nitrogen profiles of the soils. *J Soil Sci* 4(2): 143-&. <https://doi.org/10.1111/j.1365-2389.1953.tb00650.x>
- Fang XM (1994) The origin and provenance of Malan loess from the eastern edge of Tibetan plateau and its adjacent areas. *Sci China Series B-Chem* 24 (5): 539-546. (In Chinese).
- Fang XM, Lu LQ, Mason JA, et al. (2003) Pedogenic response to millennial summer monsoon enhancements on the Tibetan Plateau. *Quat Int* 106: 79-88. [https://doi.org/10.1016/S1040-6182\(02\)00163-5](https://doi.org/10.1016/S1040-6182(02)00163-5)

- Gan JJ, Han W, Chun T, et al. (2015) Mechanism and characteristics of multiple catastrophic mudslides of tasi ditch in Li county of Sichuan Province. *J Cata* 30(4): 59-63. (In Chinese).
- Guggenberger G, Baumler R, Zech W, (1998) Weathering of soils developed in eolian material overlaying glacial deposits in Eastern Nepal. *Soil Sci* 163(4): 325-337.
<https://doi.org/10.1097/00010694-199804000-00007>
- Guzzetti F, Mondini AC, Cardinali M, et al (2012) Landslide inventory maps: new tools for an old problem. *Earth Sci Rev* 112 (1-2): 42-66.
<https://doi.org/10.1016/j.earscirev.2012.02.001>
- Han Y, Huh Y, Derry L (2015) Ge/Si ratios indicating hydrothermal and sulfide weathering input to rivers of the Eastern Tibetan Plateau and Mt. Baekdu. *Chem Geol* 410: 40-52.
<https://doi.org/10.1016/j.chemgeo.2015.06.001>
- Harden JW (1982) A quantitative index of soil development from field descriptions: examples from a chronosequence in central California. *Geoderma* 28(1): 1-28.
[https://doi.org/10.1016/0016-7061\(82\)90037-4](https://doi.org/10.1016/0016-7061(82)90037-4)
- Harnois L (1988) The CIW Index: a new chemical index of weathering. *Sediment Geol* 55(3-4):319-322.
[https://doi.org/10.1016/0037-0738\(88\)90137-6](https://doi.org/10.1016/0037-0738(88)90137-6)
- Hassink J (1997) The capacity of soils to preserve organic C and N by their association with clay and silt particles. *Plant Soil* 191: 77-87.
<https://doi.org/10.1023/A:1004213929699>
- Hemingway JD, Hilton RG, Hovius N, et al. (2018) Microbial oxidation of lithospheric organic carbon in rapidly eroding tropical mountain soils. *Science* 360 (6385): 209-212.
<https://doi.org/10.1126/science.aa06463>
- Hilton RG, Meunier P, Hovius N, et al. (2011) Landslide impact on organic carbon cycling in a temperate montane forest. *Earth Surf Process Landf* 36(12): 1670-1679.
<https://doi.org/10.1002/esp.2191>
- Holloway JM, Dahlgren RA (2002) Nitrogen in rock: occurrences and biogeochemical implications. *Global Biogeochem Cycles* 16(4): 65-71.
<https://doi.org/10.1029/2002GB001862>
- Huang CM and Gong ZT (2001) Quantitative studies on development of tropical soils: A case study in northern Hainan Island. *Earth science: Journal of China University of Geosciences* 26(3):315-321. (In Chinese).
- Huang CM, Gong ZT, Yang DY (2002) Genesis of soils derived from basalt in northern Hainan Island II Iron oxides *Acta Pedologica Sinica* 39(4):449-457. (In Chinese).
- Huang ZG, Zhang WQ, Chen JH, et al. (1996) China Southern red weathering crust. Beijing Ocean Press. pp 38-304.
- Huggett RJ (1998) Soil chronosequences, soil development, and soil evolution: a critical review. *Catena* 32(3-4): 155-172.
[https://doi.org/10.1016/S0341-8162\(98\)00053-8](https://doi.org/10.1016/S0341-8162(98)00053-8)
- Izquierdo JE, Houlton BZ, Van HTL (2013) Evidence for progressive phosphorus limitation over long-term ecosystem development: examination of a biogeochemical paradigm. *Plant Soil* 367(1-2): 135-147.
<https://doi.org/10.1007/s11104-013-1683-3>
- James LA (1988) Rates of organic carbon accumulation in young mineral soils Near Burroughs Glacier, Glacier Bay, Alaska. *Phys Geogr.* 9(1): 50-70.
<https://doi.org/10.1080/02723646.1988.10642339>
- Janzen HH, Fixen PE, Franzluebbers AJ, et al. (2011) Global prospects rooted in soil science. *Soil Sci Soc Am J* 75 (1): 1-8.
<https://doi.org/10.2136/sssaj2009.0216>
- Jenny H (1969) The Pygmy forest-Podsol ecosystem and its dune associates of the Mendocino Coast. *Madrono* 20(2): 60-74.
<http://creativecommons.org/licenses/by-nc/3.0/>
- Kouno K, Tuchiya Y, Ando T (1995) Measurement of soil microbial biomass phosphorus by an anion-exchange membrane method. *Soil Biol Biochem* 27(10): 1353-1357.
[https://doi.org/10.1016/0038-0717\(95\)00057-L](https://doi.org/10.1016/0038-0717(95)00057-L)
- Lichter J (1998) Primary succession and forest development on coastal Lake Michigan sand dunes. *Ecol Monogr* 68(4): 487-510.
<https://doi.org/10.2307/2657151>
- Lu HH, Yi GH, Zhang TB, et al. (2021) Variations in vegetation cue with climate change and human activity during growing seasons in the Western Sichuan Plateau, China. *Remote Sens Lett* 12(5): 419-428.
<https://doi.org/10.1080/2150704X.2021.1895447>
- Lugo AE and Brown S (1993) Management of tropical soils as sinks or sources of atmospheric carbon. *Plant Soil* 149(1): 27-41.
<https://doi.org/10.1007/BF00010760>
- Martha CE, Ryan B, David V, et al. (2008) A soil chronosequence study of the Reno valley, Italy: Insights into the relative role of climate versus anthropogenic forcing on hillslope processes during the mid-Holocene. *Geoderma* 147(3): 97-107.
<https://doi.org/10.1016/j.geoderma.2008.07.011>
- Murphy J and Riley JP (1962) A modified single solution method for the determination of phosphate in natural waters. *Anal Chim Acta* 27: 31-36.
[https://doi.org/10.1016/S0003-2670\(00\)88444-5](https://doi.org/10.1016/S0003-2670(00)88444-5)
- Nesbitt H, Young GM (1984) Prediction of some weathering trends of plutonic and volcanic rocks based on thermodynamic and kinetic considerations. *Geochim Cosmochim Acta* 48(7): 1523-1534.
[https://doi.org/10.1016/0016-7037\(84\)90408-3](https://doi.org/10.1016/0016-7037(84)90408-3)
- Nesbitt HW, Young GM (1982) Early proterozoic climate sand plate motions inferred from major element chemistry of lutites. *Nature* 299(5885):715-717.
<https://doi.org/10.1038/299715a0>
- Newman GS, Hart SC (2015) Shifting soil resource limitations and ecosystem retrogression across a three million year semi-arid substrate age gradient. *Biogeochemistry* 124(1-3): 177-186.
<https://doi.org/10.1007/s10533-015-0090-7>
- Newman GS, Coble AA, Haskins, KE et al. (2020) The expanding role of deep roots during long-term terrestrial ecosystem development. *Biogeochemistry* 108(6): 2256-2269.
<https://doi.org/10.1111/1365-2745.13444>
- Nie GZ, Gao JG, Deng Y (2004) Preliminary study on earthquake-induced dammed lake. *Q Sci* 24(3): 293-301. (In Chinese)
- Olivia R, Dirk W (2022) Landslides: An emerging model for ecosystem and soil chronosequence research. *Earth Sci Rev* 231: 104064.
<https://doi.org/10.1016/j.earscirev.2022.104064>
- Parker A (1970) An index of weathering for silicate rocks. *Geol Mag* 107(5): 501-50.
<https://doi.org/10.1017/S0016756800058581>
- Peltzer DA, Wardle DA, Allison VJ, et al. (2010) Understanding ecosystem retrogression. *Ecol Monogr* 80(4): 509-529.
<https://doi.org/10.1890/09-1552.1>
- Poelau C, Don A, Vesterdal L, et al. (2011) Temporal dynamics of soil organic carbon after land-use change in the temperate zone e carbon response functions as a model approach. *Glob Change Biol* 17(7): 2415-2427.
<https://doi.org/10.1111/j.1365-2486.2011.02408.x>
- Post WM, Kwon KC (2000) Soil carbon sequestration and land-use change: processes and potential. *Glob Change Biol* 6(8): 317-327.
<https://doi.org/10.1046/j.1365-2486.2000.00308.x>
- R Core Team (2016) R: A Language and Environment for Statistical Computing. R Foundation for Statistical Computing, Vienna.
- Ramos CE, Castellanos EJ, Restrepo C (2012) The transfer of modern organic carbon by landslide activity in tropical montane ecosystems. *J Geophys Res Atmos* 117 (G3): 2553-2554.
<https://doi.org/10.1029/2011JG001838>
- Razak KA, Santangelo M, Van CJ, et al. (2013) Generating an

- optimal dtm from airborne laser scanning data for landslide mapping in a tropical forest environment. *Geomorphology* 190(15): 112-125.
<https://doi.org/10.1016/j.geomorph.2013.02.021>
- Reimer PJ, Edouard BB, Alex BB, et al. (2013) IntCal13 and marine 13 radiocarbon age calibration curves 0-50,000 years cal BP. *Radiocarbon* 55(4): 1869-1887.
https://doi.org/10.2458/azu_js_rc.55.16947
- Rode AA (1961) The soil forming process and soil evolution. Israel Program for Scientific Translations, Jerusalem, Israel.
- Schlögel R, Malet JP, Reichenbach P, et al. (2015) Analysis of a landslide multi-date inventory in a complex mountain landscape: the ubaye valley case study. *Nat Hazards Earth Syst Sci* 3 (3): 2051-2098.
<https://doi.org/10.5194/nhessd-3-2051-2015>
- Schulz S, Brankatschk R, DÜMig A, et al. (2013) The role of microorganisms at different stages of ecosystem development for soil formation. *Biogeosciences* 10 (6): 3983-3996.
<https://doi.org/10.5194/bg-10-3983-2013>
- Selmants PC, Hart SC (2010) Phosphorus and soil development: does the walker and syers model apply to semiarid ecosystems? *Ecology* 91(2): 474-484.
<https://doi.org/10.1890/09-0243.1>
- Six J, Conant RT, Paul EA, et al. (2002) Stabilization mechanisms of soil organic matter: implications for c-saturation of soils. *Plant Soil* 241(2): 155-176.
<https://doi.org/10.1023/A:1016125726789>
- Stevens PR and Walker TW (1970) The chronosequence concept and soil formation. *Q Rev Biol* 45(4): 333-350.
<https://doi.org/10.1086/406646>
- Stewart CE, Paustian K, Conant RT, et al. (2007) Soil Carbon saturation: concept, evidence and evaluation. *Biogeochemistry* 86(1): 19-31.
<https://doi.org/10.1007/s10533-007-9140-0>
- Turner BL and Laliberté E (2015) Soil development and nutrient availability along a 2 million-year coastal dune chronosequence under species-rich mediterranean shrubland in Southwestern Australia. *Ecosystems* 18(2): 287-309.
<https://doi.org/10.1007/s10021-014-9830-0>
- Turner BL, Condrón LM, Richardson SJ, et al. (2007) Soil organic phosphorus transformations during pedogenesis. *Ecosystems* 10(7): 1166-1181.
<https://doi.org/10.1007/s10021-007-9086-z>
- Turner BL, Condrón LM, Wells A, et al. (2012) Soil Nutrient dynamics during podzol development under lowland temperature rain forest in New Zealand. *Catena* 97: 50-62.
<https://doi.org/10.1016/j.catena.2012.05.007>
- Vindušková O, Pánek T, Frouz J (2019) Soil C, N and P Dynamics along a 13 ka chronosequence of landslides under semi-natural temperate forest. *Q Sci Rev* 213(1): 18-29.
<https://doi.org/10.1016/j.quascirev.2019.04.001>
- Vitousek PM, Farrington H (1997) Nutrient limitation and soil development: Experimental test of a biogeochemical theory. *Biogeochemistry* 37(1): 63-75.
<https://doi.org/10.1023/A:1005757218475>
- Vitousek PM, Porder S, Houlton BZ, et al. (2004) Terrestrial phosphorus limitation: mechanisms, implications, and nitrogen phosphorus interactions. *Ecol Appl* 20(1): 5-15.
<https://doi.org/10.1890/08-0127.1>
- Vreeken WJ (1975) Principal kinds of chronosequences and their significance in soil history. *Soil Sci* 26(4): 378-394.
<https://doi.org/10.1111/j.1365-2389.1975.tb01962.x>
- Walker TK, Syers JK (1976) The fate of phosphorus during pedogenesis. *Geoderma* 15(1): 1-19.
[https://doi.org/10.1016/0016-7061\(76\)90066-5](https://doi.org/10.1016/0016-7061(76)90066-5)
- Walker LR, Wardle DA, Bardgett RD, et al. (2010) The use of chronosequences in studies of ecological succession and soil development. *J Ecol* 98 (4), 725-736.
<https://doi.org/10.1111/j.1365-2745.2010.01664.x>
- Wang LS, Wang XQ, Xu XN, et al. (2007) What happened on the upstream of Minjiang River in Sichuan Province 20000 years ago? *Earth Sci Front* 14(4): 189-196 (In Chinese).
- Wang SG, Wang CH, Zhang JS, et al. (2003) Debris flow hazards in Chayuan stream of Wenchuan county, Sichuan Province on August 9, 2003. *Mountain Science* 21(5): 635-637. (In Chinese)
- Wardle DA, Lawrence RW, Bardgett RD (2004) Ecosystem properties and forest decline in contrasting long-term chronosequences. *Science* 308(5772): 633c-633c.
<https://doi.org/10.1126/science.1109723>
- Wu YH, Zhou J, Bing HJ, et al. (2015) Rapid loss of phosphorus during early pedogenesis along a glacier retreat chronosequence, Gongga Mountain (Sw China). *Peerj* 3(1-2): 26557441.
<https://doi.org/10.1126/10.7717/peerj.1377>
- Xie H, Zhong DL, Li Y, et al. (2004) Features of debris flows in the upper reaches of the Changjiang River. *Resources and Environment in the Yangtze Basin* 13(1): 94-99. (In Chinese)
- Xu Q, Li WL, Dong XJ, et al. (2017) The Xinmocun landslide on June 24, 2017 in Maoxian, Sichuan: characteristics and failure mechanism. *Chinese Journal of Rock Mechanics and Engineering* 36(11): 2612-2628. (In Chinese)
- Yaalon DH (1983) Climate, time and soil development. In: Wilding LP, Smeck NE, Hall GF (eds.), *Pedogenesis and Soil Taxonomy: I. Concepts and Interactions*. Elsevier, Amsterdam, pp 223-251.
- Yang L, Luo P, Wen L, et al. (2016) Soil organic carbon accumulation during post-agricultural succession in a karst area, Southwest China. *Sci Rep* 6(1): 37118.
<https://doi.org/10.1038/srep37118>
- Yang X, Post WM (2011) Phosphorus transformations as a function of pedogenesis: a synthesis of soil phosphorus data using Hedley fractionation method. *Biogeosci Discuss* 8(10): 5907-5934.
<https://doi.org/10.5194/bg-8-2907-2011>
- Yang Y, Li D, Zhang G, et al. (2010) Evolution of consequential soils derived from volcanic basalt on tropical leizhou peninsula, South China. *Acta Pedologica Sinica* 47(5): 123-136. (In Chinese)
- Zhao QG, Wang ZQ, Liu ZL (1983) Preliminary studies on genetic properties of the allitic soils in China. *Acta Pedologica Sinica* 20(4):334-345. (In Chinese)
- Zhong J, Li S, Li Z, et al. (2022) Metamorphic fluxes of water and carbon in rivers of the Eastern Qinghai-Tibetan Plateau. *Sci China Earth Sci* 65(4): 652-661.
<https://doi.org/10.1007/s11430-021-9873-7>